COMMUNICATIONS PHYSICS

ARTICLE

https://doi.org/10.1038/s42005-020-0387-2 OPEN

Nonlocal chiral symmetry breaking in curvilinear magnetic shells

Denis D. Sheka [1✉], Oleksandr V. Pylypovskyi [1,2], Pedro Landeros [3,4], Yuri Gaididei[5], Attila Kákay[2] & Denys Makarov [2✉]

The concept of curvature and chirality in space and time are foundational for the understanding of the organic life and formation of matter in the Universe. Chiral interactions but also curvature effects are tacitly accepted to be local. A prototypical condensed matter example is a local spin-orbit- or curvature-induced Rashba or Dzyaloshinskii-Moriya interactions. Here, we introduce a chiral effect, which is essentially nonlocal and resembles itself even in static spin textures living in curvilinear magnetic nanoshells. Its physical origin is the nonlocal magnetostatic interaction. To identify this interaction, we put forth a self-consistent micromagnetic framework of curvilinear magnetism. Understanding of the nonlocal physics of curved magnetic shells requires a curvature-induced geometrical charge, which couples the magnetic sub-system with the curvilinear geometry. The chiral interaction brings about a nonlocal chiral symmetry breaking effect: it introduces handedness in an intrinsically achiral material and enables the design of magnetolectric and ferrotoroidic responses.

[1] Taras Shevchenko National University of Kyiv, Kyiv 01601, Ukraine. [2] Helmholtz-Zentrum Dresden-Rossendorf e.V., Institute of Ion Beam Physics and Materials Research, Dresden 01328, Germany. [3] Departamento de Física, Universidad Técnica Federico Santa María, Avenida España, Valparaíso 1680, Chile. [4] Center for the Development of Nanoscience and Nanotechnology (CEDENNA), Santiago 917-0124, Chile. [5] Bogolyubov Institute for Theoretical Physics of National Academy of Sciences of Ukraine, Kyiv 03680, Ukraine. ✉email: sheka@knu.ua; d.makarov@hzdr.de

The behavior of any physical system from cosmological objects in field theories[1] through living organisms in biology[2] up to synthetic objects in condensed[3] and soft[4] matter is determined by the order parameter that lives in spacetime. The spatial distribution of the order parameter is governed by the geometry of the physical space of the object, in particular its dimensionality and curvature[5,6]. As the order parameter and fields are local quantities, it is natural to approach the description of curvilinear-geometry-induced effects based on theories, which involve local interactions only. For many systems, if not for all, this local description is incomplete as nonlocal interactions naturally appear in gravity theory[7], quantum information science (quantum nonlocality and entanglement)[8], response theory in electrodynamics[9] and magnetism[10,11]. The interplay of the order parameter of magnetically ordered materials (magnetization) with the curvilinear geometry is still described at the level when local and nonlocal interactions are treated separately[12]. This makes the description of the systems inherently incomplete as the theory fails to describe the impact of curvature effects on the statics and dynamics of micromagnetic textures like magnetic domains, skyrmion bubbles and vortices.

Here, we present a micromagnetic framework of curvilinear magnetism. The theory describes the impact of curvature-induced effects, driven by both local[13] and nonlocal[14,15] interactions, on the statics and dynamics of magnetic textures in extended curved thin shells. Fundamentally, we report nonlocal chiral symmetry-breaking effect revealing itself even in statics, which does not exist in flat thin films (compare Fig. 1a–h). To understand the nonlocal physics in curved thin shells, we go beyond the established physical picture relying on surface and volume magnetostatic charges (Fig. 1i). We demonstrate that the interactions in geometrically curved thin shells unveil themselves in full by involving three fictitious mathematical constructions in the description. In the spirit of the seminal work by Brown[10], we name them magnetostatic charges now consisting of a surface charge and two charges originated from the divergence of magnetization, which is classically referred to as a volume charge. According to their geometrical properties, we term them tangential charge and geometrical charge (compare Fig. 1i, j). Being determined by the tangential magnetization components only, the tangential charge coincides with the volume charge in flat films. The geometrical charge is determined by local characteristics of the curved surface and properties of the magnetic texture. In contrast to surface and

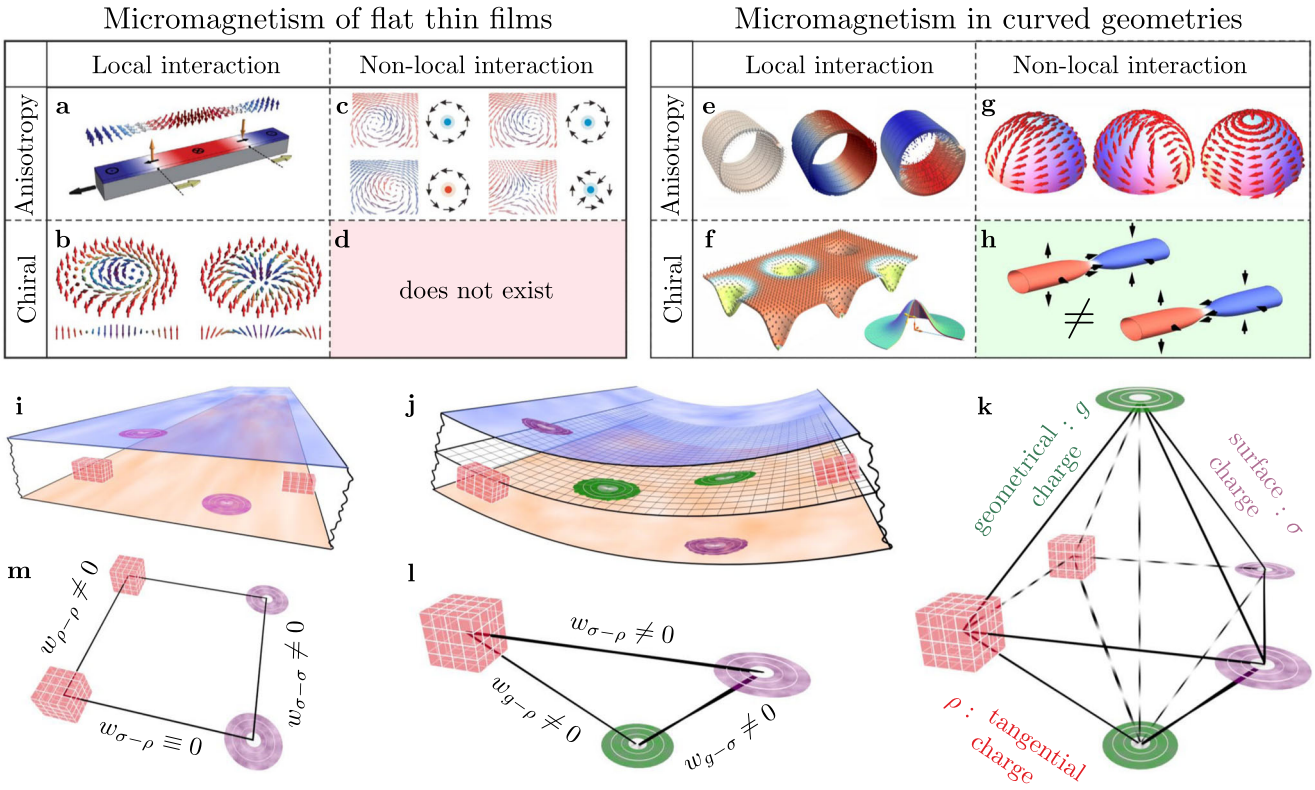

Fig. 1 Micromagnetism of static magnetization texture in flat and curved thin shells. Local spin–orbit interaction and symmetry breaking at the interfaces lead to the appearance of anisotropy (**a**)[54], and chiral terms (**b**)[55], in the energy functional of a magnetic thin film. Geometrically broken symmetry in curved magnetic shells brings about emergent anisotropy (**e**)[56], and chiral (**f**)[57], terms stemming from local exchange interaction. Nonlocal magnetostatic interaction can be reduced to a shape anisotropy in the case of thin flat (**c**)[58], and curved (**g**)[59], magnetic shells. Chiral symmetry-breaking effects stemming from nonlocal magnetostatics do not exist in statics in the case of flat thin films. **d** We report nonlocal chiral symmetry-breaking effect in curvilinear magnetic shells: **h** representative example, where nonlocal chiral symmetry breaking leads to the selection of the handedness of the Neel domain wall in a complex 3D curved out-of-plane magnetized shell. **i** Nonlocal magnetostatic interactions in the case of flat thin films can be described in the framework of Brown[10] using two fictitious charges: surface (pink shaded disks) and volume (red-shaded body). **j** The nonlocal physics in curved shells can be understood relying on three chargers: in addition to surface charge, it is insightful to introduce tangential (red-shaded body) and geometrical charges (green-shaded disks); in flat films tangential charge coincides with the volume charge. **k**, **l** All three charges do interact pairwise with a nontrivial contribution to the energy. **m** In flat films, the interaction between surface and volume charges vanishes. Panel (**a**) reprinted by permission from Springer Nature, Nature Materials[54]; (**b**) reprinted by permission from Springer Nature, Nature Materials[55]; (**c**) reprinted by permission from Springer Nature, Nature[58]; (**e**) reprinted with permission from ref. [56] copyright (2011) by the American Physical Society; (**f**) reprinted with permission from ref. [57] copyright (2018) by the American Physical Society; (**g**) reprinted with permission from ref. [59] copyright (2012) by the American Physical Society.

tangential charges, this newcomer resembles the coupling of the magnetic subsystem and geometrical curvature. We demonstrate that in geometrically curved systems, all three charges do interact pairwise with nontrivial contribution to the total energy (compare Fig. 1k–m). The nonlocal chiral symmetry-breaking effect in static magnetic textures is not only unexplored, it is not even expected in thin flat geometries. We are convinced that its analysis will stimulate the use of curved films to realize chiral magnets for fundamentally appealing and technologically relevant skyrmionic spin–orbitronic systems. The impact of this work goes well beyond the magnetism community. The presented approach can be extended for studying the evolution of generic vector fields on curved shells in different models of condensed (graphene[16] and superconductors[17]) and soft (nematics[18] and cholesterics[19]) matter.

Results

Magnetostatics of a curvilinear shell. We consider a curved ferromagnetic shell of thickness h. Its shape is locally described by Gaussian $\mathcal{K}(\mathbf{r})$ and mean $\mathcal{H}(\mathbf{r})$ curvatures. Shells are described as an extrusion of a surface $\boldsymbol{\varsigma}(\mathbf{r})$ by a constant value h along the vector $\hat{\mathbf{n}} = \hat{\mathbf{n}}(\mathbf{r})$ normal to the surface. We assume that the magnetization does not depend on the thickness coordinate along $\hat{\mathbf{n}}$. Our model includes exchange, anisotropy, and magnetostatic interactions in the energy functional. To separate the explicit curvature effects from the spurious effects of the curvilinear reference frame, it is imperative to choose the Darboux reference frame along the principal axes (see Supplementary Note 1 for details). This allows to adapt the language of covariant derivatives used in general relativity to the case of thin-shell condensed matter systems. Accounting for local intrinsic interactions only (exchange and anisotropy) allows to identify emergent curvature-induced interactions, i.e., anisotropy and Dzyaloshinskii–Moriya interaction (DMI)[13,20]. These interactions are essentially local and already widely explored for the prediction of chiral effects in curved wires and shells[12,21,22].

Following the same formalism but taking into consideration the nonlocal magnetostatic interaction, we identify the first striking property: in contrast to a flat thin film, the transformation in a curvilinear frame requires that the divergence of magnetization $\mathbf{m}$ is determined not only by the spatial derivatives of the magnetization, which determine the tangential charge ρ, but also by a new geometrical magnetostatic charge g, representing coupling of the magnetic texture and curvature

$$-\nabla\cdot\mathbf{m} = \rho + g,\qquad \rho(\mathbf{r}) = -\eth_i m_i \equiv -\eth_\alpha m_\alpha,\qquad g(\mathbf{r}) = \mathcal{H}(\mathbf{r})m_n(\mathbf{r}). \tag{1}$$

The symbol $\eth$ defines the modified tangential derivatives of magnetization in curvilinear reference frame, $\mathbf{m} = m_i\mathbf{e}_i \equiv m_\alpha\mathbf{e}_\alpha + m_n\hat{\mathbf{n}}$, with tangential components m_α and the normal component m_n; $\mathcal{H}$ is the mean curvature, which describes locally the shape of the curved shell. The geometrical charge vanishes for flat films and minimal surfaces (with $\mathcal{H}\equiv 0$) or for tangential magnetic texture with $m_n = 0$.

The geometrical charge leads to the appearance of physical effects that are intrinsically nonlocal and reveal themselves in nonlocal symmetry breaking. The geometrically broken symmetry due to the curvature results in the reorganization of the magnetostatic energy terms in the form, adapted to the geometry

$$E_\mathrm{d} = M_\mathrm{s}^2\int \mathrm{d}S w_{\sigma-\sigma} + M_\mathrm{s}^2\int \mathrm{d}\mathbf{r} w_{\rho-\rho} \tag{2A}$$

$$+M_\mathrm{s}^2\int \mathrm{d}\mathbf{r}\Big(w_{g-\sigma} + w_{g-g} + w_{g-\rho} + w_{\sigma-\rho}\Big), \tag{2B}$$

where M_s is the saturation magnetization. The first two terms (2A) are similar to the planar case

$$w_{\sigma-\sigma} = \frac{\sigma(\mathbf{r})}{2}\int\frac{\sigma(\mathbf{r}')\mathrm{d}S'}{|\mathbf{r}-\mathbf{r}'|},\quad w_{\rho-\rho} = \frac{\rho(\mathbf{r})}{2}\int \mathrm{d}\mathbf{r}'\frac{\rho(\mathbf{r}')}{|\mathbf{r}-\mathbf{r}'|}. \tag{2C}$$

Here, $w_{\sigma-\sigma}$ describes the interaction between the surfaces charges $\sigma^\pm = \mathbf{m}\cdot\mathbf{n}^\pm$ at the top/bottom surfaces of the shell. In the main order on the shell thickness h, this surface term is local, $w_{\sigma-\sigma} = (h/2)(\mathbf{m}\cdot\hat{\mathbf{n}})^2 + \mathcal{O}(h)$[23,24], and typically leads to the renormalization of anisotropy coefficients. It is the only term, linear in h stemming from the magnetostatic interaction. All other contributions to the magnetostatic interaction are essentially nonlocal[23–25]. In the thin-shell limit, they scale as $\mathcal{O}(h)$.

The magnetostatic terms $w_{g-\sigma}$ and w_{g-g} describe the interaction between geometrical and surface charges, and the interaction between geometrical charges, respectively

$$w_{g-\sigma} = g(\mathbf{r})\int\frac{\sigma(\mathbf{r}')\mathrm{d}S'}{|\mathbf{r}-\mathbf{r}'|},\quad w_{g-g} = \frac{g(\mathbf{r})}{2}\int\frac{g(\mathbf{r}')\mathrm{d}\mathbf{r}'}{|\mathbf{r}-\mathbf{r}'|}. \tag{2D}$$

Both contributions provide nonlocal coupling between normal magnetization components. The interaction between the geometrical and tangential charges

$$w_{g-\rho} = \rho(\mathbf{r})\int\frac{g(\mathbf{r}')\mathrm{d}\mathbf{r}'}{|\mathbf{r}-\mathbf{r}'|}, \tag{2E}$$

favors the coupling between the normal magnetization m_n and spatial derivatives of the in-surface components m_α. Another magnetostatic term of similar symmetry

$$w_{\sigma-\rho} = \rho(\mathbf{r})\int\frac{\sigma(\mathbf{r}')\mathrm{d}S'}{|\mathbf{r}-\mathbf{r}'|}, \tag{2F}$$

is caused by the interaction between magnetostatic surface and tangential charges. We note that this term does not contribute to the total energy of extended flat thin films (Fig. 1m, $w_{\sigma-\rho}\equiv 0$). Among others, $w_{\sigma-\rho}$ naturally appears in cylindrical and spherical shells due to the difference in the area of the inner and outer surfaces. Both interactions $w_{g-\rho}$ and $w_{\sigma-\rho}$ vanish for any homogeneous magnetic texture in a curved shell.

In addition to the established curvature-induced local anisotropy and chiral terms, driven by the exchange interaction[13,20], the nonlocal symmetry breaking of magnetic textures discussed in the following section, stems from the magnetostatic interaction. Understanding of nonlocal physics in curvilinear shells naturally involves three magnetostatic charges: surface, tangential, and geometrical charges (Fig. 1k). The latter one is determined by the mean curvature $\mathcal{H}$ coupled to the magnetic texture. In flat thin films, the interaction between volume ρ and surface σ charges does not contribute to the energy: taking into account that magnetization does not depend on the normal coordinate, surface charges on opposite surfaces of any flat thin film will compensate each other; the term (Eq. 2F) gives necessarily zero contribution to the energy density of a thin film, $w_{\sigma-\rho}^\mathrm{flat}\equiv 0$ (Fig. 1m). In contrast, in curved magnetic shells, these symmetry operations (i.e., mirror symmetry about the curved surface) are absent, hence $w_{\sigma-\rho}\neq 0$ for inhomogeneous textures (Fig. 1k, l).

Symmetry-breaking effects. The pair interactions between three charges, ρ, σ, and g, result in symmetry-breaking effects. Different energy contributions (Eqs. 2D–F) have different spatial and magnetic symmetries. First, the magnetic symmetry of $w_{g-\sigma}$ and w_{g-g} preserves the mirror symmetry of the magnetic texture about the curved surface, and therefore cannot lead to chiral effects.

Two other terms, $w_{g-\rho}$ and $w_{\sigma-\rho}$, favor a coupling between the normal magnetization component and the direction of the gradient of the in-surface magnetization components. For

Surface		Local characteristics of a surface			Anisotropy		Local interactions			Non-local interactions			Texture symmetry
		κ_1	κ_2	Surface element	Type	$\mathbf{e}_a$	$w_A^\times$	$w_{D1}^\times$	$w_{D2}^\times$	$w_{g-\sigma}$ & w_{g-g}	$w_{g-\rho}$	$w_{\sigma-\rho}$	
Developable, $\mathcal{K}=0$	Generalized cylinders (elliptical cylinders, ripples etc.)	0	$\kappa_2(x_2)$	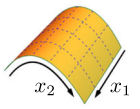	easy-axis	$\hat{\mathbf{n}}$, $\mathbf{e}_2$	✓	–	✓	✓	✓	✓	$\mathbf{m}(x_2)$
					hard-axis	$\hat{\mathbf{n}}$	✓	–	–	–	–	–	$\mathbf{m}=\mathbf{e}_1$
					easy-axis	$\mathbf{e}_1$							
					easy-axis or hard-axis	$\mathbf{e}_a$	✓	–	✓	✓	✓	✓	$\mathbf{m}(x_1,x_2)$
	Circular cylinder	0	const	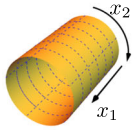	easy-axis	$\hat{\mathbf{n}}$	✓	–	–	✓	–	–	$\mathbf{m}=\hat{\mathbf{n}}$
					hard-axis	$\hat{\mathbf{n}}$	✓	–	–	–	–	–	$\mathbf{m}=\mathbf{e}_1$
					easy-axis	$\mathbf{e}_1$							
					easy-axis	$\mathbf{e}_2$	✓	–	–	–	–	–	$\mathbf{m}=\mathbf{e}_2$
Minimal, $\mathcal{H}=0$	Minimal surface	$\kappa_1(x_1,x_2)$	$-\kappa_1(x_1,x_2)$	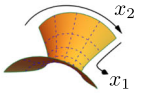	easy-axis or hard-axis	$\mathbf{e}_a$	✓	✓	✓	–	–	✓	$\mathbf{m}(x_1,x_2)$
	Catenoid	$\kappa_1(x_1)$	$-\kappa_1(x_1)$	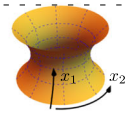	easy-axis	$\hat{\mathbf{n}}$, $\mathbf{e}_1$	✓	✓	✓	–	–	✓	$\mathbf{m}(x_1)$
General case, $\mathcal{K}\neq 0$, $\mathcal{H}\neq 0$	A curvilinear shell	$\kappa_1(x_1,x_2)$	$\kappa_2(x_1,x_2)$	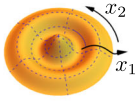	easy-axis or hard-axis	$\mathbf{e}_a$	✓	✓	✓	✓	✓	✓	$\mathbf{m}(x_1,x_2)$
	Sphere	$\kappa_1=\kappa_2=$ const		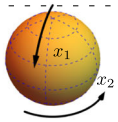	easy-axis	$\hat{\mathbf{n}}$	✓	–	–	✓	–	–	$\mathbf{m}=\hat{\mathbf{n}}$
					easy-axis or hard-axis	$\mathbf{e}_a$	✓	✓	✓	✓	✓	✓	$\mathbf{m}(x_1,x_2)$

Fig. 2 Interplay between symmetry of magnetic interactions, curvature, and magnetic texture. Effects of curvature-induced interactions on assumed equilibrium state $\widetilde{\mathbf{m}}$ given by the anisotropy for different symmetries. Here, each of the curvatures is considered either zero or nonconstant function. We consider that the respective energy term will impact the texture if the term is nonzero. The central and right-hand parts of the figure contain consequences of the input given on the left. A direction $\mathbf{e}_a$ is one of the unit vectors or their linear combination.

instance, due to the $w_{g-\rho}$ term, and for the case $m_n \neq 0$ and $\partial_\alpha m_\alpha > 0$, the magnetization favors tilt outward the surface for positive mean curvatures, $\mathcal{H}>0$, and inward for $\mathcal{H}<0$. The symmetry of these terms supports chiral symmetry breaking yet in specific cases. The sufficient conditions to admit the nonlocal chiral symmetry breaking about the x_1 axis can be formulated as follows: (i) existence of a symmetry about a flat mirror in Cartesian frame about one of the principal axis x_1 for a curved shell, (ii) the magnetic texture needs to have both out-of-surface components m_n and spatially inhomogeneous in-surface magnetic texture at least along x_1, and (iii) the magnetization components m_n and m_α should be of different parity with respect to the reflection $x_1 \to -x_1$. These conditions can be satisfied for noncollinear magnetic textures like domain walls not only for a class of developable surfaces (Fig. 2), e.g., a generalized cylinder with generatrix x_1, but also for a complex curvilinear shell as an elliptic cylinder shell with a bottleneck shown in Fig. 1h. Such surfaces provide preferential direction x_1, which can act as a possible chiral axis for the magnetization texture. Depending on the geometry and material parameters, one of the possible equilibrium states is the normally magnetized shell. We emphasize that this is an assumed ground state that is a subject of further modifications due to local and nonlocal curvilinear effects. With respect to the modifications of this assumed state due to the local interaction (see Fig. 2): local anisotropy together with local chiral effects will lead to the appearance of the azimuthal component $m_2(x_2)$. In accordance with the above analysis, there will be a nonlocal chiral symmetry breaking for the Neel domain wall: two domain walls (along and opposite x_1) are energetically not equivalent, see Fig. 1h. In this respect, the nonlocal chiral symmetry breaking is similar to its local counterpart, the DMI: the sign of DMI vector determines whether right-handed or left-handed canting between the two spins is the lower energy configuration. This is how the local DMI as well as the nonlocal chiral symmetry breaking can favor homochiral spin textures with one handedness over the other[26]. This is the first prediction of chiral symmetry breaking stemming from nonlocal interactions in static magnetic textures.

Although there are striking similarities with intrinsic DMI and curvature-induced exchange-driven DMI (both are local interactions), the nonlocal chiral symmetry breaking possesses essential fundamental differences. Namely, the symmetry of local chiral interaction terms is dictated by Lifshitz invariants, possessing properties similar to the antisymmetric curl operator. Therefore, there appear twists on the magnetic texture in Dzyaloshinskii spirals in 1D wires[27], chiral[28] and transverse[29] domain walls in flat nanostripes with intrinsic DMI, or twists in transverse[30] and periodic[31] domain walls in quasi-1D magnetic helices. Instead,

the nonlocal chiral symmetry breaking originates from the pair interaction of tangential, surface, and geometrical charges. The differential properties, caused by the tangential charges, are similar to the surface divergence operator, which does not support twists on the magnetic texture.

Discussion

The developed micromagnetism of curvilinear shells allows to make generic predictions on how the properties of magnetic textures will change, depending on the type of curved surface they live in. Considering magnetic shells with strong uniaxial anisotropy, we can readily perform analysis of textures, which do not deviate significantly from the assumed equilibrium state stabilized by the magnetocrystalline anisotropy. We can assess if the resulting magnetic texture will be modified due to the presence of a curvature-induced anisotropy and if the texture is chiral. In this respect, we analyze the energy contributions from local (anisotropy $w_{\mathrm{A}}^{\mathrm{x}}$ and DMI $w_{\mathrm{D1}}^{\mathrm{x}}$ and $w_{\mathrm{D2}}^{\mathrm{x}}$) and nonlocal terms (Fig. 2) accounting for local curvatures and the direction of the easy axis in the vicinity of a given point. To illustrate the above approach, we consider a developable surface with vanishing Gaussian curvature, $\mathcal{K} = 0$, and nonconstant second principal curvature ($\kappa_1 = 0$, $\kappa_2 \neq 0$), e.g., elliptic cylinder or ripple, and assume that magnetic easy axis is pointing normally to the surface. Then, the magnetic texture $\mathbf{m} = \mathbf{m}(x_2)$ is influenced by $w_{\mathrm{D2}}^{\mathrm{x}}$ (local chiral term). Nonlocal magnetostatic terms, $w_{g-\sigma}$, w_{g-g}, and $w_{g-\rho}$, are also present since the mean curvature is nonzero. The term $w_{\sigma-\rho}$, which is responsible for the interaction between the surface and tangential charges, can appear due to inequivalence of top and bottom surfaces of the shell for inhomogeneous magnetization texture with nonvanishing tangential magnetostatic charges. Based on these considerations, the assumed equilibrium state $\widetilde{\mathbf{m}}$ (e.g., normally magnetized elliptic cylinder) will be modified due to local and nonlocal curvature effects as follows: (i) the state will be with a break of symmetry (and, possibly, chiral), i.e., deviation from the $\hat{\mathbf{n}}$ is linear with respect to $\kappa_2(x_2)$, and (ii) effective easy–normal anisotropy will be inhomogeneously changed. As a result of this consideration, the initially assumed strictly normal magnetization distribution is modified by the appearance of the m_2 component: $\mathbf{m} = \{0,\ m_2(x_2),\ m_n(x_2)\}$. Further details are described in "Methods".

The proposed theory can be used to describe not only complex static magnetic textures but also dynamic excitations. As a characteristic example, the dynamic responses of tubular and spherical architectures are discussed in Supplementary Note 1.

The magnetism in curved geometries encompasses a range of fascinating geometry-induced effects ranging from emergent anisotropy and DMI to the possibility to create new magnetoelectric responses[12,32]. Here, we put forth a platform for theoretical analysis of micromagnetic textures in curvilinear ferromagnetic shells of different geometries. The developed generalized micromagnetic framework of curvilinear ferromagnetic shells treats local (exchange and anisotropy) and nonlocal (magnetostatics) interactions on equal footing.

A direct consequence of accounting for nonlocality is the appearance of three magnetostatic charges, which do interact with each other pairwise. This interaction brings about nonlocal chiral symmetry-breaking effect. We note that this finding is not the result of adding new energy terms to the energy functional of a flat thin film. Furthermore, there is no counterpart of this mechanism in any flat system possessing the same energy functional. Similar to the established spin–orbit-induced DMI and curvature-induced local chiral interactions, the nonlocal chiral symmetry breaking leads to the stabilization of magnetic textures with preferred handedness. Still, the physical consequences of this effect are distinct from local chiral effects. While local intrinsic DMI in helimagnets causes twists in magnetic textures (as spiralization[27]), nonlocal magnetostatics results in handedness but not in the appearance of a twist. In this respect, nonlocal chiral symmetry breaking is different even from the curvature-induced DMI originating from the exchange interaction: the local exchange-driven DMI in chiral curvilinear geometries (helix[31,33], Möbius[34]) results in the appearance of a twist in a magnetic texture similar to the intrinsic DMI.

Magnetostatics influences on the magnetic textures of a thin curved shell because of the presence of shell surfaces: both face and edge ones. In the current study, we focus on the curvature effects caused by face surfaces, which is applicable for extended shells. Hence, we do not consider possible boundary effects. For instance, complex geometry of the boundary (e.g., boundary notches and curvature) can be the source of other effects, which are already widely used to control the domain wall propagation in flat stripes with complex boundaries[35–37], and formation of vortices in magnetically soft disks[38]. The reason is that boundary effects result in complementary but not the same ways to the symmetry breaking in magnetic textures. Here we discuss only the effects, related to point geometrical characteristics, fundamentally important for curvilinear shells.

The nonlocal chiral symmetry breaking is a mechanism toward tuning material responses relying on the choice of the geometry in contrast to the conventional route of the optimization of material properties. The possibility to stabilize the preferred handedness of a nonlocal magnetic texture, e.g., the domain wall in the intrinsically not chiral magnets even in statics is technologically relevant for current-driven domain wall motion in racetrack memory[39,40] and domain wall logic devices[41]. The broken time-reversal and space-inversion symmetries in curved magnetic shells are fundamentally appealing for the realization of exotic materials possessing ferrotoroidic order[42] and design of magnetoelectric responses in geometrically curved but still conventional ferromagnetic thin films. These appealing predictions are yet to be explored theoretically and in experiments.

The impact of this work goes beyond the magnetism community. The approach toward the description of a generic vector field can be applied in various emergent fields of studies of curvature effects in condensed and soft matter. Among the prospective application, there are modification of local electronic properties of a twisted graphene bilayer induced by a strain and a high curvature[16], the evolution of the electron spin orientation $\mathbf{d}$ vector in curved superconducting nanostructures[43], domain texture, described by the polarization vector in flexible ferroelectric inorganic[44] and organic[45] crystals, and manipulation of molecule alignment in liquid crystals[18], including the effect of curvature on defects and assembly[46].

Methods

Magnetic interactions in curvilinear geometries. We consider a model of ferromagnetic shell with magnetic texture controlled by the exchange, anisotropy, and magnetostatic interactions. The total energy has the following form:

$$\begin{aligned} E &= E^{\mathrm{x}} + E^{\mathrm{an}} + E^{\mathrm{d}},\\ E^{\mathrm{x}} &= -A\int \mathrm{d}\mathbf{r}\ \mathbf{m}\cdot\nabla^2\mathbf{m},\\ E^{\mathrm{an}} &= \frac{K}{2}\int \mathrm{d}\mathbf{r}(\mathbf{m}\cdot\mathbf{e}_{\mathrm{a}})^2,\\ E^{\mathrm{d}} &= \frac{M_{\mathrm{s}}^2}{2}\int \mathrm{d}\mathbf{r}\int \mathrm{d}\mathbf{r}'(\mathbf{m}(\mathbf{r})\cdot\nabla)(\mathbf{m}(\mathbf{r}')\cdot\nabla')\frac{1}{|\mathbf{r}-\mathbf{r}'|}, \end{aligned} \tag{3}$$

where A is the exchange stiffness and K is the constant of uniaxial anisotropy. We suppose that the anisotropy direction $\mathbf{e}_{\mathrm{a}}$ is determined by the surface geometry, it corresponds to one of the principal directions or their linear combination, and m_n is the normal component of magnetization, see also Supplementary Note 2. By choosing the curvilinear reference frame, adapted to the geometry of an object, anisotropy obtains its usual spatially invariant form.

We generalize the description of magnetic curvilinear shells by introducing tangential derivatives of unit magnetization vector $\mathbf{m} = \mathbf{M}/M_s$ defined as the following:

$$\eth_\alpha m_\beta := \frac{\partial_\alpha m_\beta + \epsilon_{\beta\gamma}(\mathbf{e}_1 \cdot \partial_\alpha \mathbf{e}_2) m_\gamma}{\sqrt{\mathfrak{g}_{\alpha\alpha}}}, \qquad \eth_\alpha m_n := \frac{\partial_\alpha m_n}{\sqrt{\mathfrak{g}_{\alpha\alpha}}}, \quad \alpha, \beta = 1, 2. \tag{4}$$

Here, $\mathfrak{g}_{\alpha\beta}$ is metric tensor and $\epsilon_{\beta\gamma}$ is totally antisymmetric tensor, m_i is an ith magnetization component in the curvilinear orthonormal Darboux three-frame $\{\mathbf{e}_1, \mathbf{e}_2, \hat{\mathbf{n}}\}$ on the surface $\boldsymbol{\varsigma}$, where $\mathbf{e}_1$ and $\mathbf{e}_2$ are unit vectors corresponding to the principal directions, see Supplementary Note 2 for details. We use Greek letters $\alpha, \beta, \ldots = 1, 2$ to denote indices restricted to the shell surface. To indicate all three components of any vector, we use Latin indices $i, j, \ldots = 1, 2, n$. The Einstein summation convention is also used.

The main purpose of using this language is to separate two effects: a system-specific curvature effect and spurious effect of the curvilinear reference frame. Because of the geometry-broken symmetry, it is natural to restructure all magnetic energy terms containing spatial derivatives. A characteristic example is an exchange interaction: being isotropic in the Cartesian reference frame, it contains three components of different symmetries in curvilinear coordinates, $E^{\mathrm{x}} = E^{\mathrm{x}}_0 + E^{\mathrm{x}}_{\mathrm{A}} + E^{\mathrm{x}}_{\mathrm{D}}$[13,47]. Here, E^{x}_0 is a "common," regular isotropic part of exchange interaction, which has the form similar to the one in a planar film

$$E^{\mathrm{x}}_0 = Ah \int (\eth_\alpha m_i)(\eth_\alpha m_i) \mathrm{d}S. \tag{5A}$$

We emphasize that all effects that stem from the choice of the reference frame are properly and unambiguously assigned to E^{x}_0. This represents the major advantage of the approach based on tangential derivatives.

The second term in the exchange energy reads

$$E^{\mathrm{x}}_{\mathrm{A}} = Ah \int w^{\mathrm{x}}_{\mathrm{A}} \mathrm{d}S, \quad w^{\mathrm{x}}_{\mathrm{A}} = \mathscr{K}_{ij} m_i m_j. \tag{5B}$$

In general, this energy term describes the curvature-induced biaxial anisotropy, $\left\| \mathscr{K}_{ij} \right\| = \mathrm{diag}(\kappa_1^2, \kappa_2^2, \kappa_1^2 + \kappa_2^2)$ with κ_1 and κ_2 being local values of principal curvatures related to Gaussian and mean curvature as $\mathcal{K} = \kappa_1 \kappa_2$ and $\mathcal{H} = \kappa_1 + \kappa_2$, respectively. A striking manifestation of the curvature-induced anisotropy is shape-induced patterning, for a review see ref. [12]. The last term in the exchange energy is a curvature-induced chiral interaction (extrinsic DMI)[13]

$$E^{\mathrm{x}}_{\mathrm{D}} = Ah \int \mathrm{d}S\left(w^{\mathrm{x}}_{\mathrm{D}1} + w^{\mathrm{x}}_{\mathrm{D}2}\right), \quad w^{\mathrm{x}}_{\mathrm{D}\alpha} = 2\kappa_\alpha \mathscr{L}^{(\alpha)}_{an}, \tag{5C}$$

where no summation over α in Eq. (5C) is applied. This term is determined by the curvilinear-geometry analog of Lifshitz invariants

$$\mathscr{L}^{(\alpha)}_{ij} = m_i \partial_\alpha m_j - m_j \partial_\alpha m_i. \tag{5D}$$

The two Lifshitz invariants in (5C) are determined by principal curvatures κ_1 and κ_2. The curvature-induced DMI is a reason for a local chiral symmetry breaking, i.e., magnetochiral effects[15], for a review see ref. [12].

Classification of curvature effects by shell type. A direct analysis of all magnetostatic energy contributions (Eq. 2A) is complicated by the nonlocal integration kernels. For this reason, we apply a symmetry analysis to the energy of a ferromagnetic shell to distinguish sources of possible effects of curvature on the magnetic texture.

In the following, we consider the case of strong anisotropies, which allows us to study a magnetic texture, which does not deviate significantly from the assumed equilibrium state $\widetilde{\mathbf{m}}$ given by the anisotropy. We are interested in how local properties, i.e., local curvatures of the surface and local orientation of the magnetic easy axis, impact the resulting global magnetic state.

For our discussion, we consider uniaxial magnets with special types of anisotropy along one of the principal directions for the following distinct cases of surfaces:

(i) A class of developable surfaces of zero Gaussian curvature, $\mathcal{K}(\mathbf{r}) = 0$, includes cylinders, cones, and tangent surfaces[48]. They can be locally developed into a plane without stretching. Since cones and tangent surfaces are singular ones[49], here, we consider generalized cylindrical surfaces only.
(ii) Minimal surfaces with vanishing mean curvature, $\mathcal{H}(\mathbf{r}) = 0$, have principal curvatures of opposite signs, and in the vicinity of each point, they are saddle-shaped. Minimal surfaces provide the minimal surface area enclosed by a given boundary.
(iii) General case with nonvanishing $\mathcal{H}$ and $\mathcal{K}$ and arbitrary local surface elements, including convex and saddle ones.

The impact of the geometry on a magnetic texture is summarized in Fig. 2. It is given by the interplay of the curvature-induced energy terms and the type of anisotropy and orientation of the anisotropy axis. We refer to the curvature-related energy terms as the following:

$$E = E_0 + Ah \int \mathrm{d}S\left(w^{\mathrm{x}}_{\mathrm{A}} + w^{\mathrm{x}}_{\mathrm{D}1} + w^{\mathrm{x}}_{\mathrm{D}2}\right) + M_s^2 \int \mathrm{d}\mathbf{r}\left(w_{g-\sigma} + w_{g-g} + w_{g-\rho} + w_{\sigma-\rho}\right). \tag{6}$$

Here, $E_0 = E^{\mathrm{x}}_0 + E^{\mathrm{an}}_0$ comprises terms that have the form similar to flat systems; they contain derivatives of magnetization components, and can result in symmetry breaking and chiral effects even in a purely planar case due to chiral magnetic texture, the so-called pattern-induced chirality breaking[12]. These effects are well studied for magnons on the background of solitons[50], vortices[51], and skyrmions[52].

The curvature-induced exchange terms $w^{\mathrm{x}}_{\mathrm{A}}$, $w^{\mathrm{x}}_{\mathrm{D}1}$, and $w^{\mathrm{x}}_{\mathrm{D}2}$ scale linearly with the shell thickness. Magnetostatic terms $w_{g-\sigma}$, w_{g-g}, and $w_{g-\rho}$ are present only for curved shells with a nonzero mean curvature, $\mathcal{H} \neq 0$; for the infinitesimally thin shells, they scale quadratically with thickness. These magnetostatic terms are absent for minimal surfaces, e.g., for catenoids and helicoids. The term $w_{\sigma-\rho}$ is present only for the inhomogeneous magnetization texture if top and bottom surfaces of the shell are not equivalent. It appears due to the coupling between surface and tangential magnetostatic charges $\sigma^{\pm}$ and ρ (we do not discuss here the specific picture of interaction between edge-surface charges with volume ones, which is available also in flat systems[53]).

It is important to stress that such an approach cannot be considered as a sufficient condition of existence and moreover stability of the corresponding magnetization states. No other criteria are applied with assembly in Fig. 2. Here, we discuss possible statical states by applying only symmetrical arguments to the energy functional irrelevant whether they are in local minimum of energy or not. Investigation of equilibrium magnetization texture for the concrete geometry should be a purpose of a separate work. For example, $w^{\mathrm{x}}_{\mathrm{D}1}$ does not impact magnetic textures (it vanishes) for the following cases: either $\kappa_1 \equiv 0$, or magnetic texture does not vary along x_1, or $m_n \equiv 0$. A possible magnetic texture is assumed based on the sample symmetry and interplay between intrinsic and curvature-induced anisotropies.

Minimal surfaces do not exhibit effects, which explicitly depend on the curvature due to $\mathcal{H} \equiv 0$. At the same time, all geometry-induced exchange-driven terms are present for any texture symmetry, except easy-surface anisotropy or easy-axis anisotropy along $\mathbf{e}_2$. The symmetry-broken magnetostatics-driven term $w_{\sigma-\rho}$ is always present for inhomogeneous textures with nonzero magnetostatic charge if the top and bottom surfaces of a shell are not equivalent. As in the previous case, the initially assumed strictly normal magnetic texture is modified by the appearance of the m_1 component: $\mathbf{m} = \{m_1(x_1), 0, m_n(x_1)\}$ for a catenoid.

For the general case of $\mathcal{H} \neq 0$ and $\mathcal{K} \neq 0$, all effects stemming from both local exchange and nonlocal magnetostatics interaction are possible. Note that Fig. 2 is also valid for nonlinear excitations of the equilibrium state like domain walls if their symmetry corresponds to the function given in the "Texture symmetry" column.

Data availability

The data that support the plots within this paper and other findings of this study are available from the corresponding author upon reasonable request.

Received: 1 April 2020; Accepted: 8 June 2020;
Published online: 20 July 2020

References

1. Misner, C. W., Thorne, K. S. & Wheeler, J. A. *Gravitation*. (Princeton University Press, New Jersey, 2017).
2. McMahon, H. T. & Gallop, J. L. Membrane curvature and mechanisms of dynamic cell membrane remodelling. *Nature* **438**, 590–596 (2005).
3. Castelvecchi, D. The strange topology that is reshaping physics. *Nature* **547**, 272–274 (2017).
4. Senyuk, B. et al. Topological colloids. *Nature* **493**, 200–205 (2012).
5. Bowick, M. J. & Giomi, L. Two-dimensional matter: order, curvature and defects. *Adv. Phys.* **58**, 449–563 (2009).
6. Turner, A. M., Vitelli, V. & Nelson, D. R. Vortices on curved surfaces. *Rev. Mod. Phys.* **82**, 1301–1348 (2010).
7. Mashhoon, B. *Nonlocal Gravity*. (OUP Oxford, New York, 2017).
8. Gisin, N. Quantum nonlocality: how does nature do it? *Science* **326**, 1357–1358 (2009).
9. Landau, L. D., Pitaevskii, L. P. & Lifshitz, E. M. *Electrodynamics of Continuous Media*. (Pergamon Press, Great Britain, 1984).
10. Brown, W. F., Jr *Micromagnetics*. (Wiley, New York, 1963).
11. Hubert, A. & Schäfer, R. *Magnetic Domains: The Analysis of Magnetic Microstructures* (Springer Berlin Heidelberg, Berlin, 2009).
12. Streubel, R. et al. Magnetism in curved geometries (topical review). *J. Phys. D* **49**, 363001 (2016).
13. Gaididei, Y., Kravchuk, V. P. & Sheka, D. D. Curvature effects in thin magnetic shells. *Phys. Rev. Lett.* **112**, 257203 (2014).

14. Landeros, P. & Núñez, A. S. Domain wall motion on magnetic nanotubes. *J. Appl. Phys.* **108**, 033917 (2010).
15. Hertel, R. Curvature–induced magnetochirality. *SPIN* **03**, 1340009 (2013).
16. Yan, W. et al. Strain and curvature induced evolution of electronic band structures in twisted graphene bilayer. *Nat. Commun.* **4** (2013).
17. Vitelli, V. & Turner, A. M. Anomalous coupling between topological defects and curvature. *Phys. Rev. Lett.* **93**, 215301 (2004).
18. Napoli, G. & Vergori, L. Extrinsic curvature effects on nematic shells. *Phys. Rev. Lett.* **108**, 207803 (2012).
19. Napoli, G. & Vergori, L. Effective free energies for cholesteric shells. *Soft Matter* **9**, 8378 (2013).
20. Sheka, D. D., Kravchuk, V. P., Yershov, K. V. & Gaididei, Y. Torsion-induced effects in magnetic nanowires. *Phys. Rev. B* **92**, 054417 (2015).
21. Sander, D. et al. The 2017 magnetism roadmap. *J. Phys. D* **50**, 363001 (2017).
22. Fernández-Pacheco, A. et al. Three-dimensional nanomagnetism. *Nat. Commun.* **8**, 15756 (2017).
23. Carbou, G. Thin layers in micromagnetism. *Math. Models Methods Appl. Sci. (M3AS)* **11**, 1529–1546 (2001).
24. Kohn, R. V. & Slastikov, V. V. Another thin-film limit of micromagnetics. *Arch. Ration. Mech. Anal.* **178**, 227–245 (2005).
25. Fratta, G. D., Muratov, C. B., Rybakov, F. N. & Slastikov, V. V. *Variational Principles of Micromagnetics Revisited*. http://arxiv.org/abs/1905.04568v1 (2019).
26. Chen, G. & Schmid, A. K. Imaging and tailoring the chirality of domain walls in magnetic films. *Adv. Mater.* **27**, 5738–5743 (2015).
27. Dzialoshinskii, I. E. Thermodynamic theory of "weak" ferromagnetism in antiferromagnetic substances. *Sov. Phys. JETP* **5**, 1259–1272 (1957).
28. Ryu, K.-S., Thomas, L., Yang, S.-H. & Parkin, S. Chiral spin torque at magnetic domain walls. *Nat. Nanotechnol.* **8**, 527–533 (2013).
29. Kravchuk, V. P. Influence of Dzialoshinskii–Moriya interaction on static and dynamic properties of a transverse domain wall. *J. Magn. Magn. Mater.* **367**, 9 (2014).
30. Pylypovskyi, O. V. et al. Rashba torque driven domain wall motion in magnetic helices. *Sci. Rep.* **6**, 23316 (2016).
31. Volkov, O. M. et al. Mesoscale Dzyaloshinskii-Moriya interaction: geometrical tailoring of the magnetochirality. *Sci. Rep.* **8**, 866 (2018).
32. Volkov, O. M. et al. Experimental observation of exchange-driven chiral effects in curvilinear magnetism. *Phys. Rev. Lett.* **123**, 077201 (2019).
33. Volkov, O., Rossler, U. K., Fassbender, J. & Makarov, D. Concept of artificial magnetoelectric materials via geometrically controlling curvilinear helimagnets. *J. Phys. D* **52**, 345001 (2019).
34. Pylypovskyi, O. V. et al. Coupling of chiralities in spin and physical spaces: the Möbius ring as a case study. *Phys. Rev. Lett.* **114**, 197204 (2015).
35. Kläui, M. et al. Controlled and reproducible domain wall displacement by current pulses injected into ferromagnetic ring structures. *Phys. Rev. Lett.* **94**, 106601 (2005).
36. Himeno, A. et al. Propagation of a magnetic domain wall in magnetic wires with asymmetric notches. *J. Appl. Phys.* **97**, 066101 (2005).
37. Mawass, M.-A. et al. Switching by domain-wall automotion in asymmetric ferromagnetic rings. *Phys. Rev. Appl.* **7**, 044009 (2017).
38. Okuno, T., Shigeto, K., Ono, T., Mibu, K. & Shinjo, T. MFM study of magnetic vortex cores in circular permalloy dots: behavior in external field. *J. Magn. Magn. Mater.* **240**, 1–6 (2002).
39. Parkin, S. S. P., Hayashi, M. & Thomas, L. Magnetic domain-wall racetrack memory. *Science* **320**, 190–194 (2008).
40. Fert, A., Reyren, N. & Cros, V. Magnetic skyrmions: advances in physics and potential applications. *Nat. Rev. Mater.* **2**, 17031 (2017).
41. Allwood, D. A. et al. Magnetic domain–wall logic. *Science* **309**, 1688–1692 (2005).
42. Spaldin, N. A., Fiebig, M. & Mostovoy, M. The toroidal moment in condensed-matter physics and its relation to the magnetoelectric effect. *J. Phys.* **20**, 434203 (2008).
43. Ying, Z.-J., Cuoco, M., Ortix, C. & Gentile, P. Tuning pairing amplitude and spin-triplet texture by curving superconducting nanostructures. *Phys. Rev. B* **96**, 100506(R) (2017).
44. Chang, L., You, L. & Wang, J. The path to flexible ferroelectrics: approaches and progress. *Jpn. J. Appl. Phys.* **57**, 0902A3 (2018).
45. Owczarek, M. et al. Flexible ferroelectric organic crystals. *Nat. Commun.* **7**, 13108 (2016).
46. Serra, F. Curvature and defects in nematic liquid crystals. *Liq. Cryst.* **43**, 1920–1936 (2016).
47. Sheka, D. D., Kravchuk, V. P. & Gaididei, Y. Curvature effects in statics and dynamics of low dimensional magnets. *J. Phys. A* **48**, 125202 (2015).
48. Krivoshapko, S. & Ivanov, V. *Encyclopedia of Analytical Surfaces* (Springer-Verlag GmbH, 2015).
49. Johansen, P. H. The geometry of the tangent developable. In *Computational Methods for Algebraic Spline Surfaces* (eds. Dokken, T. & Jüttler, B.) 95–106 (Springer-Verlag, 2005).
50. Sheka, D. D., Ivanov, B. A. & Mertens, F. G. Internal modes and magnon scattering on topological solitons in two–dimensional easy–axis ferromagnets. *Phys. Rev. B* **64**, 024432 (2001).
51. Sheka, D. D., Yastremsky, I. A., Ivanov, B. A., Wysin, G. M. & Mertens, F. G. Amplitudes for magnon scattering by vortices in two–dimensional weakly easy–plane ferromagnets. *Phys. Rev. B* **69**, 054429 (2004).
52. Kravchuk, V. P., Sheka, D. D., Rößler, U. K., van den Brink, J. & Gaididei, Y. Spin eigenmodes of magnetic skyrmions and the problem of the effective skyrmion mass. *Phys. Rev. B* **97**, 064403 (2018).
53. Nonaka, K., Hirono, S. & Hatakeyama, I. Magnetostatic energy of magnetic thin-film edge having volume and surface charges. *J. Appl. Phys.* **58**, 1610–1614 (1985).
54. Emori, S., Bauer, U., Ahn, S.-M., Martinez, E. & Beach, G. S. D. Current-driven dynamics of chiral ferromagnetic domain walls. *Nat. Mater.* **12**, 611–616 (2013).
55. Kézsmárki, I. et al. Néel-type skyrmion lattice with confined orientation in the polar magnetic semiconductor GaV_4S_8. *Nat. Mater.* **14**, 1116–1122 (2015).
56. Smith, E. J., Makarov, D., Sanchez, S., Fomin, V. M. & Schmidt, O. G. Magnetic microhelix coil structures. *Phys. Rev. Lett.* **107**, 097204 (2011).
57. Kravchuk, V. P. et al. Multiplet of skyrmion states on a curvilinear defect: reconfigurable skyrmion lattices. *Phys. Rev. Lett.* **120**, 067201 (2018).
58. Van Waeyenberge, B. et al. Magnetic vortex core reversal by excitation with short bursts of an alternating field. *Nature* **444**, 461–464 (2006).
59. Streubel, R. et al. Magnetic vortices on closely packed spherically curved surfaces. *Phys. Rev. B* **85**, 174429 (2012).

Acknowledgements

The authors thank Dr. Volodymyr Kravchuk (Karlsruhe Institute of Technology) for helpful discussions. D.D.S. thanks Helmholtz-Zentrum Dresden-Rossendorf e. V. (HZDR), where part of this work was performed, for their kind hospitality, and acknowledges the support from the Alexander von Humboldt Foundation (Research Group Linkage Programme). O. V.P. acknowledges the support from DAAD (Code no. 91530902). We acknowledge the support from German Research Foundation (DFG) grant MA 5144/9-1, MA 5144/14-1, MA 5144/22-1, FONDECYT 1161403, and Centers of excellence with Basal/CONICYT financing, grant AFB180001, CEDENNA. This work was partially supported by Taras Shevchenko National University of Kyiv (Projects 19BF052-01 and 18BF052-01M) and the Program of Fundamental Research of the Department of Physics and Astronomy of the National Academy of Sciences of Ukraine (Project no. 0116U003192).

Author contributions

D.D.S., O.V.P., and D.M. formulated the theoretical problem. D.D.S., O.V.P., and Y.G. developed the formalism of tangential derivatives. P.L. and A.K. contributed with the understanding of the effects in developable surfaces. D.D.S., O.V.P., and D.M. wrote the paper with the contribution from all authors. All coauthors edited the paper. D.D.S. and D.M. conceived the project.

Competing interests

The authors declare no competing interests.

Additional information

Supplementary information is available for this paper at https://doi.org/10.1038/s42005-020-0387-2.

Correspondence and requests for materials should be addressed to D.D.S. or D.M.

Reprints and permission information is available at http://www.nature.com/reprints

Publisher's note Springer Nature remains neutral with regard to jurisdictional claims in published maps and institutional affiliations.

Open Access This article is licensed under a Creative Commons Attribution 4.0 International License, which permits use, sharing, adaptation, distribution and reproduction in any medium or format, as long as you give appropriate credit to the original author(s) and the source, provide a link to the Creative Commons license, and indicate if changes were made. The images or other third party material in this article are included in the article's Creative Commons license, unless indicated otherwise in a credit line to the material. If material is not included in the article's Creative Commons license and your intended use is not permitted by statutory regulation or exceeds the permitted use, you will need to obtain permission directly from the copyright holder. To view a copy of this license, visit http://creativecommons.org/licenses/by/4.0/.

© The Author(s) 2020